Structural Engineering and Mechanics, *Vol. 72, No. 4 (2019) 479-489*
DOI: https://doi.org/10.12989/sem.2019.72.4.479

Sensitivity analysis of flexural strength of RC beams influenced by reinforcement corrosion

Seyed A. Hosseini*[1], Naser Shabakhty[2a] and Fardin Azhdary Khankahdani[3b]

[1]*Faculty of Technology and Mining, Yasouj University, Choram 75761-59836, Iran*
[2]*School of Civil Engineering, Iran university of Science and Technology, Tehran, Iran*
[3]*Department of civil engineering, Shiraz Branch, Islamic Azad University, Shiraz, Iran*

(Received September 17, 2017, Revised December 4, 2018, Accepted July 6, 2019)

Abstract. The corrosion of reinforcement leads to a gradual decay of structural strength and durability. Several models for crack occurrence prediction and crack width propagation are investigated in this paper. Analytical and experimental models were used to predict the bond strength in the period of corrosion propagation. The manner of flexural strength loss is calculated by application of these models for different scenarios. As a new approach, the variation of the concrete beam neutral axis height has been evaluated, which shows a reduction in the neutral axis height for the scenarios without loss of bond. Alternatively, an increase of the neutral axis height was observed for the scenarios including bond and concrete section loss. The statistical properties of the parameters influencing the strength have been deliberated associated with obtaining the time-dependent bending strength during corrosion propagation, using Monte Carlo (MC) random sampling method. Results showed that the ultimate strain in concrete decreases significantly as a consequence of the bond strength reduction during the corrosion process, when the section reaches to its final limit. Therefore, such sections are likely to show brittle behavior.

Keywords: reinforcement corrosion; flexural strength; bond reduction; stochastic model

1. Introduction

Reinforcement corrosion has a high importance especially in concrete buildings located in the coastal marine environments and in bridges exposed to de-icing salts. The reinforcement corrosion is mainly generated with the presence of chloride ions (Zhou *et al.* 2017). Reinforcement corrosion affects strength and serviceability of reinforced concrete (RC) structures over time as a result of the reduction in concrete and steel cross-sectional area or loss of bond between steel and concrete. Considerable researches have been performed to evaluate the effect of corrosion on the concrete structures in the past. Capozucca and Cerri (2003), investigated the influence of corrosion on the compression strength of concrete around the corroded reinforcement and introduced a reduction coefficient for the strength of concrete in different conditions. Almusallam *et al.* (1996), assessed the bond strength reduction by facilitating corrosion conditions in the total length of the beam with longitudinal reinforcements. Other researchers such as Lin and Zhao (2016) and Chung *et al.* (2008) were well studied the concrete reinforcement corrosion with creating accelerated corrosion conditions in the total length of steel reinforcement. Corrosion is a process which usually occurs gradually over time; therefore, an accelerated corrosion was used in all experiments. Some researchers have been established some samples by creating corrosion with natural speed (Vidal *et al.* 2007, Malerba *et al.* 2017). Du *et al.* (2013) have been applied permanent loads to a reinforced concrete beam when a part of reinforcement is corroded.

Durability Modeling and structural reliability evaluation of the RC structures requires a quantitative description of corrosion propagation. Uncertainties in the calculation of the damage extent related to corrosion initiation and consequence of corrosion propagation should be taken into account because of the random nature of corrosion. Time-dependent reliability methods will help to reach an optimum inspection and maintenance strategies during service life of corroded RC structures, which minimizes the future maintenance cost and keeps the failure probability at or below of the desired value. Mori and Ellingwood (1993) based on the loss of reinforcement cross-sectional area have calculated the time-dependent reliability of corroded RC beam with a simple steady-state linear time function for strength reduction. Most of the reliability assessment studies are dealing with the simple steady-state linear function of time for the loss of reinforcement cross-sectional area (Enright and Frangopol 1998, Vu *et al.* 2000). Liu and Weyers (1998) have reported the loss of reinforcement cross-sectional area may not be taken as a simple linear function. Also, this issue has been reported by other researchers (liu and Weyers 1998, Bhargava *et al.* 2005). Most of the earlier Evaluations of flexural strength of the corrosion-degraded RC structural members encounter with the bond strength of corroded reinforcement (Duprat

*Corresponding author, Assistant Professor
E-mail: a.hosseini@yu.ac.ir
[a] Assistant Professor
[b] Assistant Professor

http://www.techno-press.com/journals/sem&subpage=7
ISSN: 1225-4568 (Print), 1598-6217 (Online)

2007, Enright and Frangopol 1998). Time-dependent flexural strength with considering the bond strength have been investigated very little in the literature (Hosseini *et al.* 2015).

In spite of progress in studies concerning the different aspect of corrosion, the uncertainty in the effect of predominant parameters, dimensions and materials properties for predicting of structural strength after corrosion initiation has not well studied.

The present paper consists of probabilistic descriptions of the time-dependent flexural strength of corrosion-affected RC beams. Reinforcement cross-sectional area loss, bond loss between corroded reinforcement and concrete and concrete section loss due to cover spalling and/or delamination are three major issues related to corrosion in RC structures that were investigated in this study. Also, concrete section reduction due to the spalling of cover concrete in compression zone and delamination of cover concrete in the tension zone of the RC beam section have been considered. The effect of uncertainties connected to major variables affecting the corrosion both in combination and independent to dimensions and properties of materials has also investigated. Monte Carlo (MC) random sampling method in each time was used with the effective parameters as random variables in the problem. Strength has been measured with and without considering the effect of bond strength. The best statistical distribution of each analysis fitted, then the effect of parameters uncertainties on the coefficient of variation (CV) has been investigated.

The pressure zone status and neutral axis height changes of RC beam sections exposed to reinforcement corrosion are considered here, which have not been investigated in the previous studies at all. The effect of bond strength and concrete ultimate strain changes on the neutral axis height proliferation of beams under corrosion process are studied.

2. Corrosion

Corrosion process is, in fact, the transformation of reinforcement metal iron due to oxidation into other iron compounds. Thus, the cross-section of reinforcement reduces. The volume of produced materials is greater than the iron consumed in the corrosion process, even more than 6.5 times in some occasions, depending on the oxidation rate (liu and Weyers 1998).

As corrosion initiates, the cross-sectional area of reinforcement reduces. Pitting and general corrosion are the two most common types of steel reinforcement corrosion in concrete. Reinforcement cross-sectional area reduction rate expresses through corrosion rate (r_c), measured based on the corrosion current density, i_{cor} as shown in Eq. (1) (Enright and Frangopol, 1998).

$$r_c = 0.0116\alpha i_{cor} \tag{1}$$

where α is the type of corrosion as it is 2 for homogeneous corrosion, however, it may become 4 up to 8 in the case of the pitting occurs (Gonzales *et al.* 1995). Corrosion current density depends on local conditions such as concrete type and some other factors. Some of the main factors affecting the corrosion current density (i_{cor}) are the water-cement ratio (w/c) and concrete cover thickness. The following equation has been proposed for the corrosion current density after initiation, in relative humidity of 70% and average temperature of 20 degrees (Vu *et al.* 2000):

$$i_{cor}(I) = \frac{37.8(1-w/c)^{-1.64}}{c_c} \tag{2}$$

where c_c (cm) is the clear cover. Diameter of the corroding reinforcing bar $D(t)$ at time t, can be estimated directly from corrosion rate as Eq. (3)

$$D(t) = D_0 - \int_0^t r_c dt \tag{3}$$

where D_0 is the initial diameter of the reinforcing bar., The corrosion rate reduces after elapsing of time the amount of reduction is higher at the beginning of corrosion, gradually become slower at consequent moments (Vu *et al.* 2005). Vu *et al.* (2000) suggested the following time-dependent equation for $i_{cor}(t)$

$$i_{cor}(t) = i_{cor}(t) \times 0.85(t-T_i)^{-0.29} \tag{4}$$

where T_i is the corrosion initiation time. The reinforcement diameter (in mm) at time t can be estimated in the case of uniform corrosion by Eq. (5).

$$D(t) = D_0 - 0.0278 i_{cor}(I) \times (t-T_i)^{0.71} \tag{5}$$

where i_{cor} (I) is the initial corrosion current density.

2.1 Cracking

The volume increase causes cracking of the concrete cover and finally leading to its eventual spalling and/or delamination. Cracking time prediction and crack width calculating due to corrosion of reinforcing bars have been investigated by some researchers (Vu *et al.* 2005, Jamali *et al.* 2013). Corrosion-induced cracking models might be classified into three main approaches including empirical, analytical, and numerical. In general, at all models the crack propagation time period, t_{cr} has direct proportion to the critical amount of the corrosion products W_{cr} (e.g. g/mm^2 reinforcing bar surface) and inverse proportion to the corrosion current density, i_{cor}. Based on available information spalling and delamination are supposed to occur at a crack width of approximately 1.0 mm (Duracrete, 2000). Some researcher tried to predict corrosion crack width during propagation (Rodriguez *et al.* 1996, Vidal *et al.* 2004, Zhang *et al.* 2010, Khan *et al.* 2014) Some of the empirical models are presented in Table 1. These models are based on loss of steel cross-section.

2.2 Bond strength reduction

Reinforcement corrosion gradually influences the cohesion, adhesion, and friction between the steel-concrete

Table 1 Empirical models of crack width

Reference	Model
Rodriguez *et al.* (1996)	$w = 0.05 + \beta(x - x_0)$
Vidal *et al.* (2004)	$w = 0.0575(\Delta A_s - \Delta A_{s0})$
Zhang *et al.* (2010)	$w = 0.1916\Delta A_{sm} + 0.164$
Khan *et al.* (2014)	$w = 0.1916\Delta A_{sm} D / c + 0.164$

Notations: W: crack width (mm); β=0.01 for top cast bars and β= 0.0125 for bottom cast bars; x: reinforcement radius decrease (µm); x_o: attack penetration leading to cracking initiation (µm); c: clear cover (mm); D: reinforcement diameter (mm); ΔAs: local reinforcement cross-section loss (mm^2); ΔA_{so}: reinforcement cross-section loss for crack initiation (mm^2); ΔA_{sm}: average cross-section Loss of corroded reinforcement (mm^2);

Table 2 Empirical bond strength models

Reference	Model
Stanish *et al.* (1999)	$\tau_{bu} = (0.77 - 0.027X_p) \times \sqrt{f_c^{'}}$
Cabrera (1996)	$\tau_{bu} = 23.478 - 1.313X_p$
Lee *et al.* (2002)	$\tau_{bu} = 5.21\exp(-0.0561X_p)$
Chung *et al.* (2004)	$\tau_{bu} = 2.09X_p^{-1.06}$
Bhargava *et al.* (2007)	$\tau_{bu} = 1.192\exp(-0.117X_p)$
Chung et al. (2008)	$\tau_{bu} = 24.7X_p^{-0.55}$

interfaces. Bond strength reduction rate will be a key factor in determining the ultimate strength of corroded RC component at the desired time. A variety of studies have been performed based on reinforcement diameter size, concrete type and local conditions. Alternatively, considerable theoretical models have been proposed to describe bond strength changes (Stanish *et al.* 1999). The ultimate bond strength increases at initial stages of corrosion as a consequence of extra volume caused by corrosion due to increase in pressure around the bar (Fang *et al.* 2006). Lee *et al.* (2002) based on the reinforcement corrosion rate offered a relation to estimate the residual bond strength between the corroded reinforcement and concrete. Substantial experiments have been conducted in both direct tensile test (pullout tests) and test of tension caused by bending (flexural test) to propose an empirical model to predict the changes in bond strength reduction during corrosion propagation (Cabrera 1996, Stanish *et al.* 1999, Chung *et al.* 2004). The bond strength reduction often expresses as a percentage of the reinforcing bar mass loss compared to the original bar mass at time *t*, (X_p). Some of the empirical models are presented in Table 2.

3. Effect of corrosion on bending strength

The ultimate strength of a reinforced concrete beam $M_u(t)$ conveniently calculates with considering linear

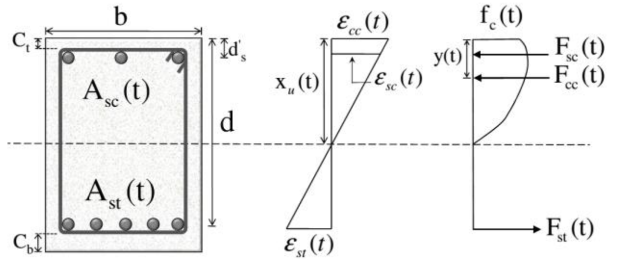

Fig. 1 Typical cross section of RC beams and stress-strain distribution

distribution of strain at beam height (cross section is shown in Fig. 1). For this beam, bending strength $M_u(t)$ is calculated as below

$$M_u(t) = F_{st}(t)\left[d(t) - y(t)\right] + F_{sc}(t)\left\lfloor y(t) - d_s^{'}(t)\right\rfloor \tag{6}$$

where $F_{sc}(t)$ and $F_{st}(t)$ are the forces in compressive and tensile steel respectively; y(t) is the distance of edge compression zone to the the compressive force centroid in concrete ($F_{cc}(t)$).

The strain in compressive steel ε_{sc} and strain in tensile steal ε_{st} at any time *t* define as follows

$$\varepsilon_{st}(t) = \left[\frac{d(t) - x_u(t)}{x_u(t)}\right]\varepsilon_{cc} \tag{7a}$$

$$\varepsilon_{sc}(t) = \left[\frac{x_u(t) - d_s^{'}(t)}{x_u(t)}\right]\varepsilon_{cc} \tag{7b}$$

where $x_u(t)$, $d(t)$, $d_u^{'}(t)$ and ε_{cc} are neutral axis height, effective depth to tensile reinforcement, effective depth to compressive reinforcement and concrete ultimate strain, respectively.

In this case, by passage of time and corrosion influence, the values including $x_u(t)$, $F_{st}(t)$ and $F_{sc}(t)$ change as a result of reinforcements cross sectional area reduction; therefore, the value of $M_u(t)$ reduces either.

As bond strength reduces, the reinforcement separation should be considered as the failure point of the cross section. To this end, if the amount of force in rebar is more than residual bond strength, the cross section failure is determined by the amount of residual bond. In designing for bending, this force is transmitted at the length of l_d which is known as development length. As reinforcement corrosion increases at this length, the amount of adhesive force reduces; this force is calculated at any time from corrosion initiation as below. This force will be the maximum force bearable by reinforcement and a limit state for the ultimate strength of the reinforced concrete section.

$$F_{st}(t) = n\pi D_{rt}(t) l_d \tau_{bu}(t) \tag{8}$$

where *n* is the number of reinforcements, $D_{rt}(t)$ is the remaining diameter of rebar and $\tau_{bu}(t)$ stands for residual bond strength in the moment *t* after corrosion initiation.

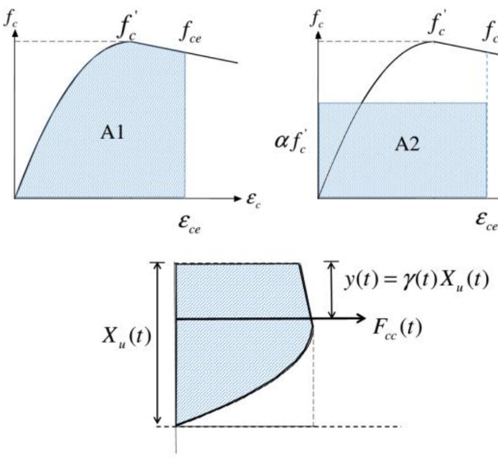

Fig. 2 Concrete stress-strain curve

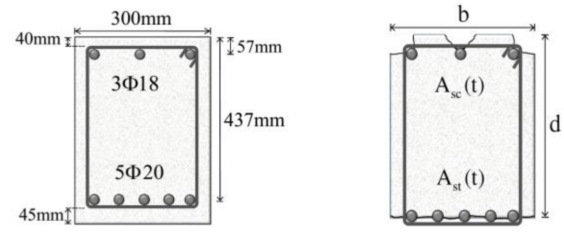

(a) (b)

Fig. 3 RC beam cross-section: (a) intact concrete section; (b) reduced concrete section due to the spalling of top and peeling bottom covers

When the maximum bearable force in tensile rebar was determined, the maximum allowable strain for rebar can be achieved:

$$\varepsilon_{st}(t)=\frac{F_{st}(t)}{A_{st}(t)E_{st}} \tag{9}$$

The strain values in the compressive steel rebar and the farthest concrete compressive axis can be achieved:

$$\varepsilon_{sc}(t)=\left[\frac{x_u(t)-d_s'(t)}{d(t)-x_u(t)}\right]\varepsilon_{st}(t) \tag{10a}$$

$$\varepsilon_{cc}(t)=\left[\frac{x_u(t)}{d(t)-x_u(t)}\right]\varepsilon_{st}(t) \tag{10b}$$

Stress distribution in concrete would be non-linear if strain surpasses half of the concrete ultimate strain, but as concrete strain might has not reached to ultimate value (0.003) when the tensile force in reinforcement reaches to the ultimate limit, hence it is not possible to use the coefficients α_1 and β_1 to convert actual stress distribution into equivalent rectangular stress block. Therefore, it will be necessary to use stress and strain relation to calculate the amount of concrete compressive force. Stress value of f_{ce} at the farthest compressive axis calculates by the following relation (Kent and Park, 1971).

$$f_{ce}=f_c'\left[2\frac{\varepsilon_{ce}}{\varepsilon_0}-\left(\frac{\varepsilon_c}{\varepsilon_0}\right)^2\right] \tag{11a}$$

$$f_{ce}=f_c'\left[1-\frac{0.15}{0.003-\varepsilon_{ce}}(\varepsilon_{ce}-\varepsilon_0)\right] \tag{11b}$$

where f_c' is the compressive strength of concrete and ε_0 and ε_{ce} are the strain corresponding to f_c' and the concrete extreme fiber compressive strain.

As shown in Fig. 2, the α factor is used to convert the non-linear stress-strain relationship into an equivalent rectangular distribution by integration of below the surface of stress curve. In this figure, A1 is the surface below the stress-strain curve when the stress at the extreme compression fiber reaches f_{ce} and A2 is the equivalent rectangular stress block. The point of action of the compressive force of concrete measured from the extreme compression fiber of concrete is written as a fraction of the neutral axis depth ($y(t)=\gamma(t)x_u(t)$). $\gamma(t)$ is calculated with the first moment of the area under the stress-strain curve.

4. Materials and methods

To investigate the effect of uncertainties in degradation of bending strength and also the effect of bond strength on changes in ultimate strength and neutral axis height, the cross-section of a simply supported RC beam shown in Fig. 3(a) is considered. The statistical parameters for material strengths, dimensions of the considered RC beam and statistical parameters for assumed corrosion condition are given in Table 3.

Appearance of the first surface cracks occurs during the first period of corrosion propagation. In addition to the loss of bond crack width reaches to the extent which causes peeling of the concrete cover in the concrete cross-section in the period of corrosion propagation. The criteria considered here for this period is growth of crack width to 1 mm. Then after, the Khan *et al*. model is used for evaluating the crack width during the propagation period. Monte Carlo random sampling was used to show the development of crack width for different values of corrosion current density for the top and bottom of the given section (Fig. 4a). Also, the cumulative distribution function (CDF) based on reaching crack width to 1 mm for this model is shown in Fig. 4(b). In this figure, the time corresponding to 0.5 for CDF, indicates the 50% or less probability for crack occurrence. In later sections the effect of loss in the concrete cross section on the flexural strength is investigated using these two figures results. Statistical uncertainty presented in the crack width values for different corrosion current densities are shown in Fig. 5. As seen, for all cases, the coefficient of variation for the crack width reaches to a fixed 0.2 value after 25 years. On the other hand, at the beginning of corrosion development the

Table 3 Statistical properties of materials and dimensions

Variable	Unit	Mean	CV	Distribution
Concrete compressive strength (f_c')	MPa	25	0.15	Normal
Yield strength of reinforcing steel (F_y)	MPa	400	0.1	Lognormal
Modulus of elasticity of steel (E_s)	MPa	2E5	0.05	lognormal
Section width(b)	mm	300	0.05	Normal
Effective depth to tensile reinforcement (d)	mm	437	0.05	Normal
Effective depth to compressive Reinforcement (d_{sc})	mm	40	0.1	Normal
Clear covers to bottom (c)	mm	45	0.1	Normal
Tensile reinforcement diameter (D_{st})	mm	20	0.1	Normal
Compressive reinforcement diameter (D_{sc})	mm	18	0.1	Normal
Corrosion initiation time(T)	Year	10	0.3	Lognormal
Corrosion Current Density(i)	$\mu A/cm^2$	1, 3, 5	0.1, 0.2, 0.3	Normal

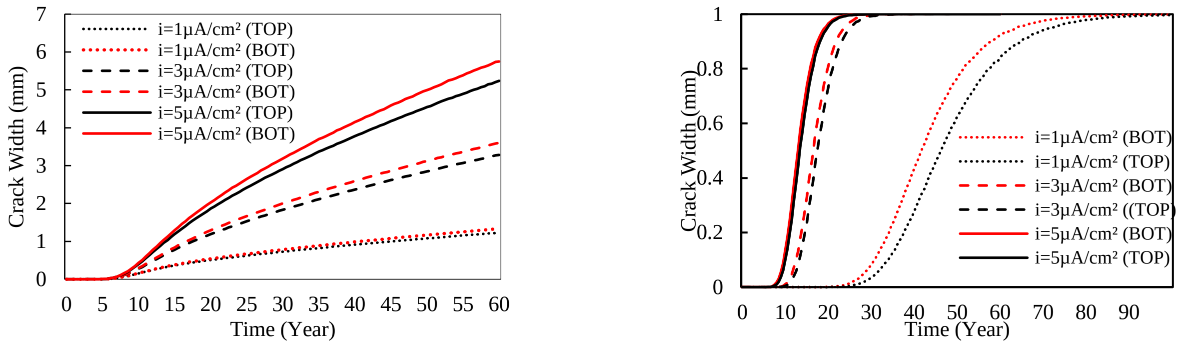

(a) (b)

Fig. 4 Application of Khan *et al.* model: (a) crack width (b) cumulative distribution function of crack width.

dispersion of the results is substantial because of the uncertainty in the corrosion initiation time. The effect of reduction in reinforcement cross section and also the effect of loss of concrete section on the flexural strength of the beam are investigated. For this purpose, at first, two different scenarios without assuming the effect of loss in bond are considered.

In the first case, only the effect of reduction in reinforcement area is considered, however in the second case, the effect of loss of concrete section on the flexural strength is considered. Flexural strength of the section is computed using MC (with 100000 samples) based on the data in Table 3 assuming Khan et al. model for the crack width at any time. As seen in Table 3, quantities 1, 3 and 5 for the corrosion current density, and 0.1, 0.2 and 0.3 for its coefficient of variation are assumed for calculation of the effect of corrosion intensity and uncertainty in parameters affecting the corrosion phenomenon.

The ratio of flexural strength at any time to initial strength (M(t)/Mo) for the two assumed scenarios and for corrosion current density 3 and different coefficients of variations are shown in Fig. 6. The results show that for both scenarios, the coefficient of variation for corrosion current density does not have any effect. Also, after reaching the crack width to its critical value (1mm), the strength shows more loss. The effect of reduction in

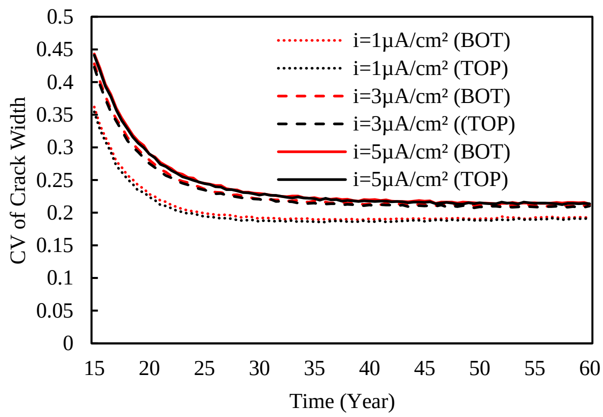

Fig. 5 Coefficient of variation of predicted crack width by Khan *et al.* (2014) model

reinforcement cross section causes 10 percent reduction in flexural strength after 50 years from the initiation of corrosion and by considering the loss of concrete section, there is only 5 percent more reduction in flexural strength. The dispersion of results, corresponding to the flexural strength are shown in Fig. 6b. The increase in uncertainty of corrosion current density had no effect on the dispersion of the results. Also for both scenarios, the coefficient of variation is almost the same and by passing of time and increase in corrosion of the bars only a small increase in the coefficient of variation of the flexural strength from 0.185

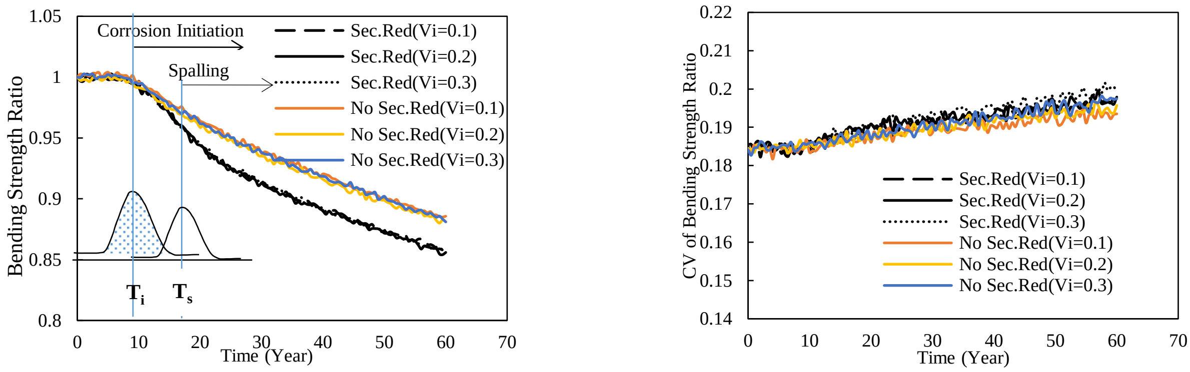

(a) (b)

Fig. 6 Time-dependent (a) mean and (b) coefficient of variation for bending strength ratio ($M(t)/M_0$) for beam section without loss of bond (i=$3\mu A/cm^2$)

to 0.195 is observed. The neutral axis height in the concrete cross-section may change due to the corrosion. As it is shown in Fig. 7, this change, depending on the conditions for establishing the balance of forces in the section, might be an increase or decrease in the height. In continuation, by assuming X_{u0} for the neutral axis height of the section before initiation of corrosion, the manner that the height of compression section of concrete changes, will be investigated.

The variation of the compression height of the concrete section (x) is shown in Fig. 8. As seen, based on the assumed scenario, two different behaviors were obtained for the neutral axis height. Without considering the effect of spalling of concrete cover, the neutral axis height reduces with time and the coefficient of variation of corrosion current density does not influence it. But when spalling of concrete is considered, the neutral axis height increases and as is evident from Fig. 8 the amount of uncertainty in corrosion current density in the domain around corrosion initiation and development of partial cracks would minor effect in the mean value of the response. The uncertainty on the determination of neutral axis height is shown in Fig. 8b. indicates a constant coefficient of variation value equal to 0.195 for the neutral axis height for the first scenario. For the second scenario within the time frame in which spalling occurs, the coefficient of variation for the neutral axis height first increases to 0.23 and then decreases to the constant value of 0.18. The percentage of variation in the neutral axis height which is calculated according to the Eq (12).

$$\Delta X_u(t) = \left| \frac{X_u(t) - X_{u0}}{X_{u0}} \right| \times 100 \tag{12}$$

where $X_u(t)$ and X_{u0} are the corrosion affected and initial neutral height of concrete beam section. $\Delta X_u(t)$ is shown in Fig. 9 for the various values of corrosion current densities. Fig. 9(a) is indicative of the percentage of reduction of the neutral axis height for the first scenario which increases by the increase of corrosion current density, so we have 13%, 8% and 3% reduction for densities of 5, 3 and 1 respectively. Fig. 9(b) shows the percentage of increase in the neutral axis height for the second scenario, which after spalling a jump in the neutral axis height is observed to make the balance with conditions of the new section. This increase reaches up to 24% of the initial height for the two values of 3 and 5 of corrosion current densities and after that start to decrease as for the first scenario. Comparing these two figures indicates that loss in the reinforcement area causes a reduction in the neutral axis height and loss in concrete section results in a jump in the neutral axis height.

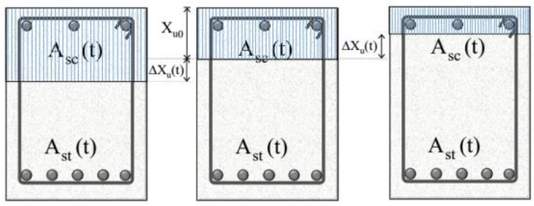

Fig. 7 The typical change in neutral height in corroded affected RC beam

In this section in order to investigate the effect of reduction in bond strength for the two previous scenarios, bond reduction during the period of corrosion propagation is assumed. For this purpose, in the first case, the effects of the reduction in the bar area and reduction of the bond is considered and for the other case in addition to the previous effects, the effect of loss of concrete section also is assumed in the calculations. First, using models introduced in Table 2, the ratio of bond loss during the period of corrosion propagation is calculated. In Fig. 10a, the diagram related to corrosion current density 3 is shown. As the percentage of bar corrosion increases during the period of corrosion propagation, bond decreases for all models. The largest and the smallest bond loss belong to the Chung et al. model and Stanish et al. model, respectively. Chung et al. (2008), Stanish et al. and Chung et al. models, represent an abrupt loss in the bond during the early stage after initiation of corrosion, but other models represent almost linear

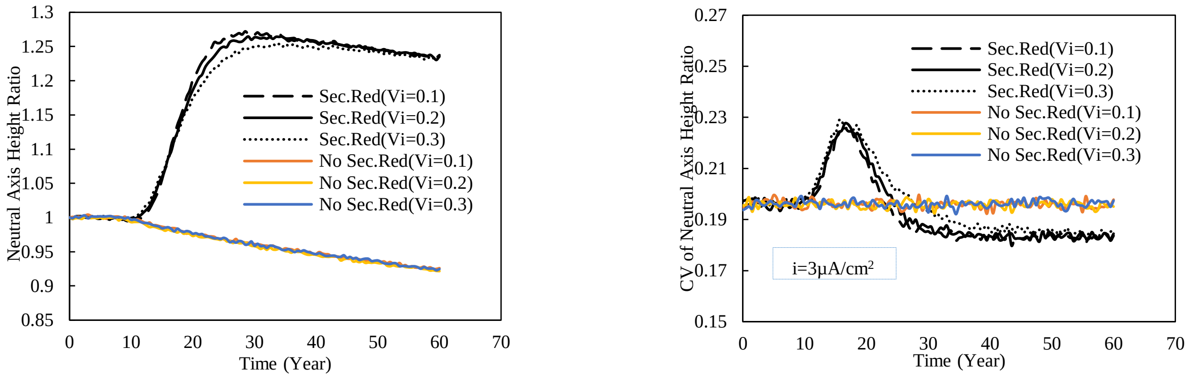

(a) (b)

Fig. 8 Time-dependent (a) mean and (b) coefficient of variation for neutral height ratio for beam section without loss of bond (i=3μA/cm²)

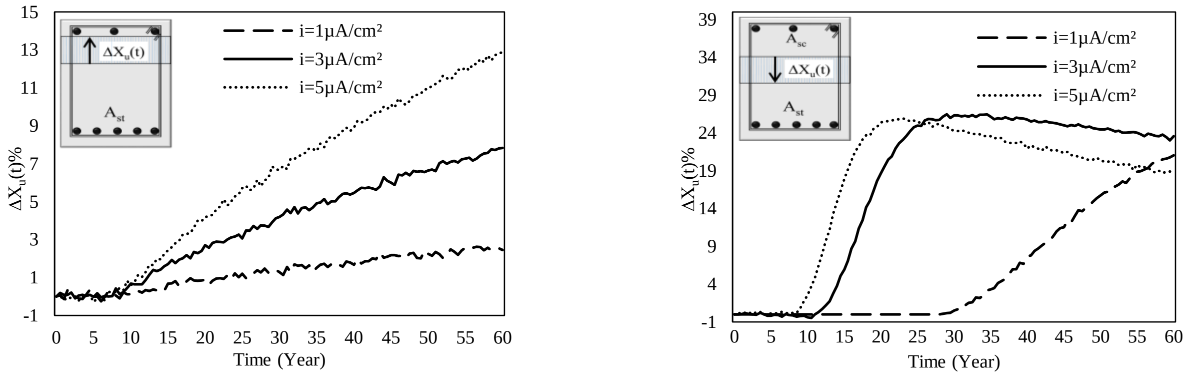

(a) (b)

Fig. 9 Time-dependent percentage of variation in the neutral axis height for cases without the loss of bond: (a) without considering concrete cross-section reduction (b) with concrete cross-section reduction

relationship during the corrosion propagation. In these models, the initial increase of bond due to the pressure of corroded material around the bar was neglected. The dispersion of bond results, based on the statistical characteristics of the effective parameters, is shown in Fig. 10(b). For most models in the initial period of bond loss, the dispersion of the results increases. This increase for Chung et al. model reaches up to 0.35 and then is reduced and tends toward the constant value of 0.15. In the two models of Stanish et al. and Cabrera, the uncertainty increases with time. These two models use a linear relationship for loss in bond and this is indicative of an increase in dispersion of corrosion percentage of bars with time.

In the following the effect of bond loss is applied for the two previous scenarios. The time-dependent flexural ratio is shown in Fig. 11(a). As seen, considering bond loss causes a substantial decrease in flexural strength compared to when there is no bond strength loss. Therefore, the flexural strength reaches 25% and 19% of initial strength for the two scenarios. This reduction, in case of no bond loss, reaches 90% and 85% for the two scenarios at the end of the 60th year (Fig. 6(a)).

The effect of corrosion current uncertainty on the flexural strength of models with bond loss is considerable. As shown in Fig. 12(b), the increase of uncertainty in corrosion current density causes an increase of dispersion of the flexural strength with time. This increase for Vi=0.30 reaches up to 0.45, while for models with no bond loss, had no effect on the dispersion of the results. From this figure also is evident that considering the loss of the concrete section had no effect on the dispersion of the flexural strength.

The effect of bond loss on variations of the neutral axis height in two cases, one assuming no loss of concrete section and the other assuming loss of concrete section is illustrated in Fig. 12(a). For both scenarios it can be seen increase in the neutral axis height, with this difference that the amount of this increase for the case of loss of concrete section is more, so that for the case of loss of cross section area this increase reaches 1.45 of initial height at the end of 60th year and for the second scenario to 1.35. As said before, the loss of the concrete section without considering the effect of bond loss causes an increase of the neutral axis height. The uncertainty in corrosion current density for the first scenario at the time domain of bond loss initiation affects the mean value of the neutral axis height ratio. This impact on the second scenario at the time domain of occurrence of spalling affects the neutral axis height. The effect of uncertainty of corrosion current density on the uncertainty of the results obtained for the neutral axis height is shown in Fig. 12b. The results indicate that they are affected by different values of coefficient of variation of

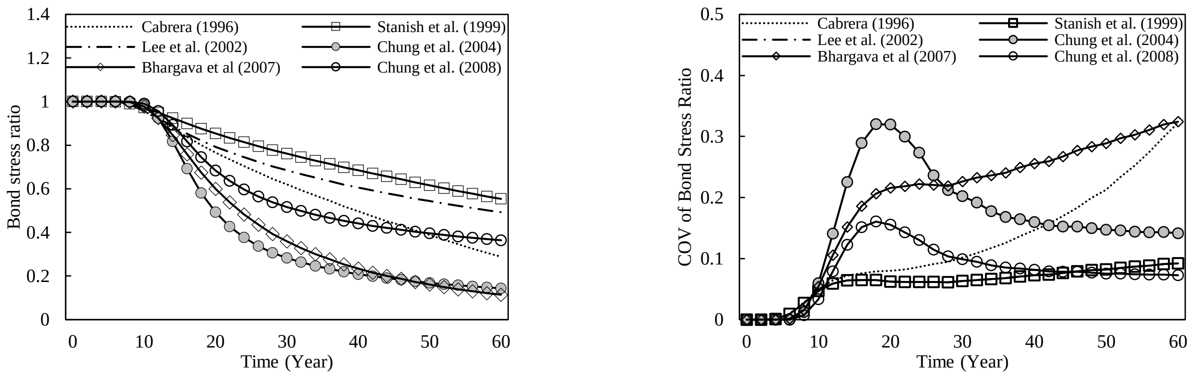

(a) (b)

Fig. 10 Time dependent (a) mean and (b) coefficient of variation of bond strength ratio (i=3μA/cm^2)

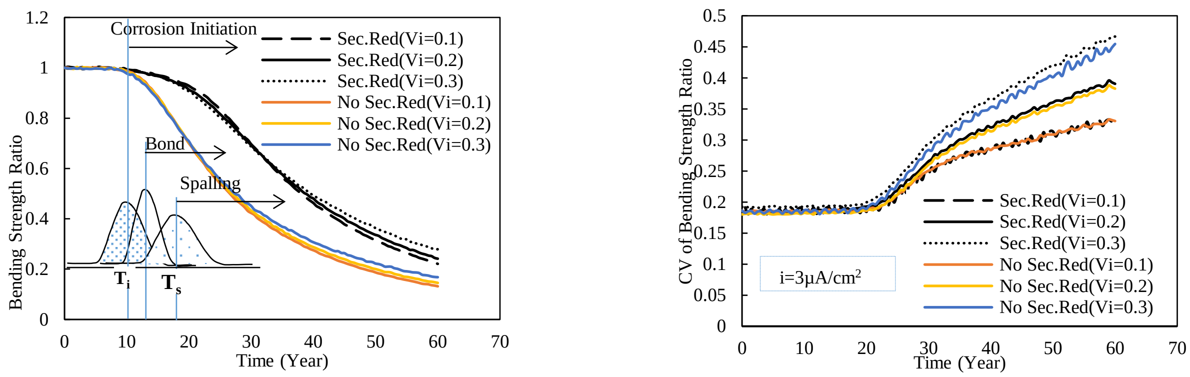

(a) (b)

Fig. 11 Time dependent (a) mean and (b) coefficient of variation for bending strength ratio (M(t)/M$_0$) of beam section with loss of bond (i=3μA/cm^2)

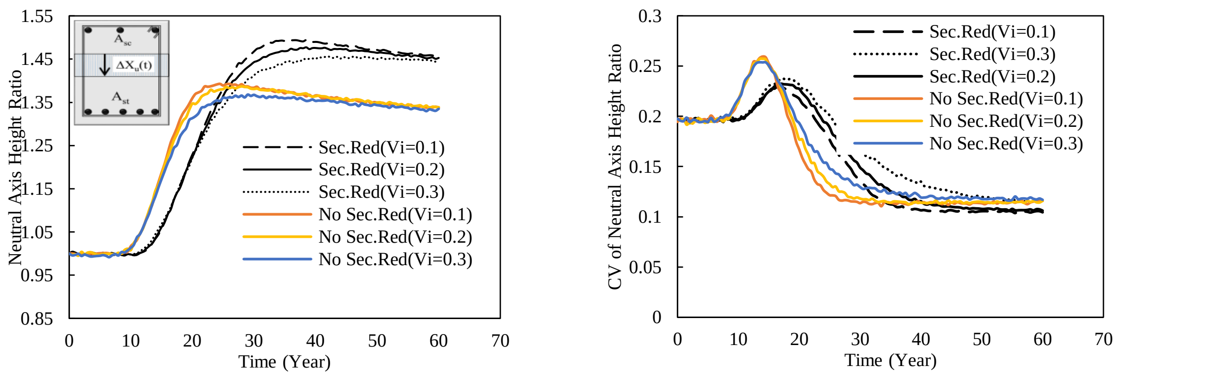

(a) (b)

Fig. 12 Time dependent (a) mean and (b) coefficient of variation of changes in the neutral axis height for beam section with loss of bond (i=3μA/cm^2)

corrosion current densities. The coefficient of variation of the neutral axis height for the time domain of bond loss initiation for the first scenario has increased in value, this is also true for the time domain of spalling development for the second scenario. This is due to the effect of existing uncertainties within models used for the prediction of bond loss and crack width determination. The important point in Fig. 12(b) is the reduction of the coefficient of variation after the initiation of bond loss and loss of concrete cross-section relative to the section before the initiation of corrosion so that coefficient of variation varies from 0.2 before corrosion initiation to 0.10 for the ultimate state of the corroded section.

The probability density function (PDF) is a useful function for expressing the random properties of a parameter. By knowing the information about the PDF of the structural resistance, its safety can be measured over time. In continuation, for the assumed previous cases, the best probability distribution function with related parameters are given. In Table 4, the obtained values of probability distribution function without loss of bond scenario, and in Table 5 with loss bond are given.

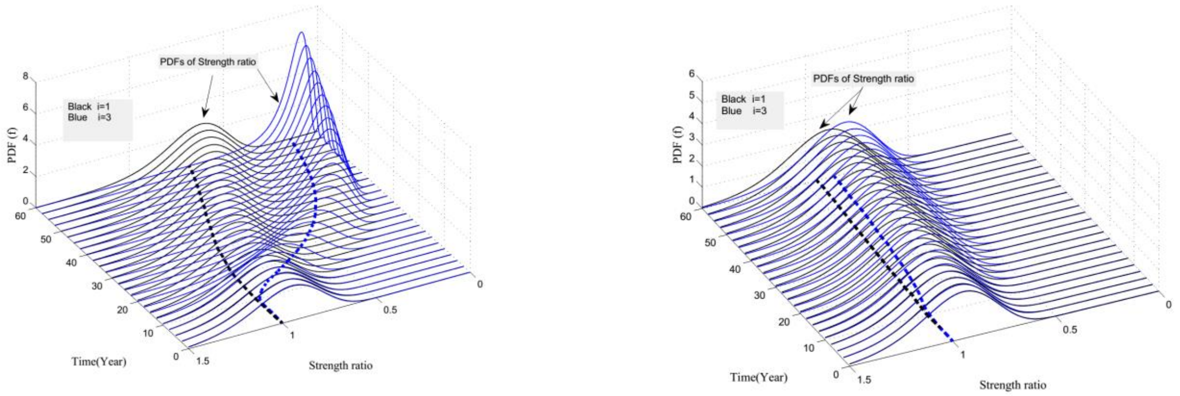

(a) (b)

Fig. 13 Fitted PDFs during corrosion propagation for flexural strength ratio: (a)

According to the results, the best probability distribution function is the three- parameter lognormal distribution which is given as Eq. (13). In this expression σ_{lnx} and μ_{lnx} are standard deviation and mean of the data, respectively and γ is the position of the data parameter. The suitability of this distribution was assessed by applying Chi-square Goodness of fit test on the available data, which is calculated based on 13 degrees of freedom and 5 percent degree of importance.

$$f(x)=\frac{1}{(x-\gamma)\sigma_{\ln x}\sqrt{2\pi}}\exp\left[-0.5\left(\frac{\ln(x-\gamma)-\mu_{\ln x}}{\sigma_{\ln x}}\right)^2\right] \quad (13)$$

Based on Chi-square standard tables related to 13 degrees of freedom and 5 percent degree of importance, it gives 22.362, If the calculated Chi-square is less than the standard value of chi-square, the fitted Distribution is acceptable. Considering values in Tables 4-5 it's clear that for this degree of importance, within the time interval of corrosion initiation, by increasing the coefficient of variation of corrosion current density, the fitted probability density function, approaches the borderline of being not acceptable. From Tables 4-5 it is evident that for cases with bond loss and cases which include loss in cross-section area in the time interval of bond loss event or reduction in cross-section area, the probability density function, with given degree of importance, is not fitted to the flexural strength and this is because of the great randomness properties associated with these parameters. In Fig. 13, the diagrams related to the ratio of reduction in the flexural strength with time together with the probability distribution functions, fitted to them are drawn. This is for better witnessed understanding of the state of changes in the fitted coefficient of variation and also its application in the reliability computations.

5. Conclusions

In this paper, effects of reinforcement corrosion including the reduction in bar and concrete cross-section area and loss of bond have been investigated in a reinforced concrete beam. Also, different models for cracking time prediction, crack width propagation determination, and bond loss between bar and concrete have been investigated. The parameters have been considered as random variables by computing probability distribution function to take into account the uncertainty effect. The assumed scenario for the loss of concrete section is based on the spalling in concrete cover in compression zone and delamination of concrete cover in the tension zone of concrete beam section. Results showed that, factors have the greatest effect on the strength reduction of the section are the bond loss, the beam cross-section reduction and finally the bar cross section reduction. As an effective factor, by increasing the development length of tensile bars, the effect of bond loss might be alleviated. Uncertainty increase in corrosion current density does not have much effect on the mean values of the flexural strength. Only in case of loss in bond, uncertainty causes an increased rate of dispersion of the results.

Table 4 Chi-square goodness of fit test for model without loss of bond

scenario	time	Vi	Distribution	Chi2 (cal)	Parameters		
					μ_{lnx}	σ_{lnx}	γ
without concrete cross-section reduction	10	0.1	LN(3p)	11.25	0.299	0.135	-.0367
		0.3	LN(3p)	21.88	0.357	0.129	-.0443
	20	0.1	LN(3p)	6.3	0.246	0.138	-0.316
		0.3	LN(3p)	3.11	0.246	0.141	-0.315
	30	0.1	LN(3p)	10.42	0.196	0.147	-0.270
		0.3	LN(3p)	17.95	0.276	0.134	-0.374
	60	0.1	LN(3p)	13.85	0.156	0.148	-0.261
		0.3	LN(3p)	20.541	0.177	0.145	-0.286
with concrete cross-section reduction	10	0.1	LN(3p)	11.25	0.30	0.135	-0.367
		0.3	LN(3p)	21.885	0.357	0.13	-0.442
	20	0.1	LN(3p)	6.51	0.271	0.135	-0.353
		0.3	LN(3p)	6.16	0.267	0.138	-0.348
	30	0.1	LN(3p)	12.78	0.223	0.141	-0.325
		0.3	LN(3p)	19.64	0.297	0.131	-0.420
	60	0.1	LN(3p)	14.45	0.182	0.142	-0.317
		0.3	LN(3p)	21.61	0.195	0.141	-0.33

Table 5 Chi-square goodness of fit test for model with loss of bond

scenario	time	Vi	Distribution	Chi2 (cal)	Parameters		
					μ_{lnx}	σ_{lnx}	γ
with concrete cross-section reduction	10	0.1	LN(3p)	10.64	0.286	0.137	-0.351
		0.3	LN(3p)	12.89	0.318	0.133	-0.392
	20	0.1	LN(3p)	16.44	0.136	0.141	-0.274
		0.3	LN(3p)	11.73	0.737	0.089	-1.22
	30	0.1	LN(3p)	6.19	-0.135	0.165	-0.23
		0.3	LN(3p)	28.33	0.167	0.171	-0.532
	60	0.1	LN(3p)	10.39	-1.07	0.249	-0.057
		0.3	LN(3p)	10.54	-1.172	0.506	-0.023
without concrete cross-section reduction	10	0.1	LN(3p)	8.04	0.357	0.130	-0.439
		0.3	LN(3p)	6.97	0.264	0.139	-0.317
	20	0.1	LN(3p)	9.15	0.288	0.122	-0.455
		0.3	LN(3p)	6.8	0.793	0.082	-1.34
	30	0.1	LN(3p)	9.28	0.067	0.137	-0.413
		0.3	LN(3p)	32.6	0.139	0.175	-0.496
	60	0.1	LN(3p)	11.83	-0.898	0.210	-0.118
		0.3	LN(3p)	8.31	-1.136	0.494	-0.030

As a most important results the pattern of neutral axis height changes, which initiate with bond loss and occurrence of spalling in the section, increases the neutral axis height to accommodate the balance of forces in the section and then reduces with a slow rate. But without loss of bond and spalling, the neutral axis height decreases during the corrosion period. Three-Parameter lognormal distribution is the best probability function to state the uncertainties of the diagram of the flexural strength reduction during the period of corrosion propagation. Although this distribution within time domain of spalling occurrence for higher values of uncertainties of corrosion current density does have some errors.

References

ACI 318 (2011), Building code requirements for structural concrete and commentary, American Concrete Institute; Farmington Hills, MI, USA.

Al-Osta, M.A., Al-Sakkaf, H.A., Sharif, A.M., Ahmad, S. and Baluch, M.H. (2018), "Finite element modeling of corroded RC beams using cohesive surface bonding approach", *Comput. Concrete,* **22**(2), 167-182. https://doi.org/10.12989/cac.2018.22.2.167.

Almusallam, A.A., Al-gahtani, A.S., Aziz, A.R. and Uzzafar, R. (1996), "Effect of reinforcement corrosion on bond strength" *Construct. Build. Mater.*, **10** (2),123–129. https://doi.org/10.1016/0950-0618(95)00077-1.

Azad, A.K., Ahmad, S. and Azher, S.A. (2007), "Residual strength of corrosion-damaged reinforcement concrete beams", *ACI Mater. J.*, **104**(1), 40-47.

Bhargava, K., Ghosh, A.K., Mori, Y. and Ramanujam, S. (2007), "Corrosion-induced bond strength degradation in reinforced concrete—Analytical and empirical models", *Nuclear Eng. Design*, **237**, 1140–1157. https://doi.org/10.1016/j.nucengdes.2007.01.010.

Cabrera, J.G. (1996), "Deterioration of concrete due to reinforcement steel corrosion", *Cem. Concr. Compos.*, **18**(1), 47–59.

Capozucca, R. and Cerri, M.N. (2003), "Influence of reinforcement corrosion in the compressive zone on the behavior of RC beams", *Eng. Struct.,* **25**(13), 1575-1583. https://doi.org/10.1016/S0141-0296(03)00119-6.

Chung, L., Cho, S.H., Kim, J.H.J. and Yi, S.T. (2004), "Correction factor suggestion for ACI development length provisions based on flexural testing of RC slabs with various levels of corroded reinforcing bars", *Eng. Struct.*, **26**(8), 1013-1026. https://doi.org/10.1016/j.engstruct.2004.01.008.

Chung, L., Kim, J.J. and Yi, S. (2008), "Bond strength prediction for reinforcement concrete with highly corroded reinforcement bars", *Cement Concrete Compos.*, **30**, 603-611. https://doi.org/10.1016/j.cemconcomp.2008.03.006.

Chung, L., Najm, H. and Balaguru, P. (2008), "Flexural behavior of concrete slabs with corroded bars", *Cement Concrete Compos.*, **30**(3), 184-193. https://doi.org/10.1016/j.cemconcomp.2007.08.005.

Du, Y., Culle, M. and Li, C. (2013), "Structural effects of simultaneous loading and reinforcement corrosion on performance of concrete beams", *Construct. Build. Mater.*, **39**, 148-152. https://doi.org/10.1016/j.conbuildmat.2012.05.006.

Duprat, F. (2007), "Reliability of RC beams under chloride-ingress", *Construct. Build. Mater.*, **21**, 1605-1616. https://doi.org/10.1016/j.conbuildmat.2006.08.002.

DuraCrete (2000), "The European Union—Brite EuRam III, DuraCrete", Technical Report, Document BE95-1347/R172000.

Enright, M.P and Frangopol, D.M. (1998), "Service-life prediction of deteriorating concrete structures", *J. Struct. Eng.,* **124**(3), 309-317. https://doi.org/10.1061/(ASCE)0733-9445(1998)124:3(309).

Enright, M.P. and Frangopol, D.M. (1998), "Probabilistic analysis of resistance degradation of reinforced concrete bridge beams under corrosion", *Eng. Struct.,* **20**(11), 960–971. https://doi.org/10.1016/S0141-0296(97)00190-9.

Fang, C., Lundgren, K., Plos, M. and Gylltoft, K. (2006), "Bond behavior of corroded reinforcing steel bars in concrete", *Cem. Concr. Res.*, **36**(10), 1931-1938. https://doi.org/10.1016/j.cemconres.2006.05.008.

Gonzales, J.A., Andrade, C., Alonso, C. and Feliu, S. (1995), "Comparison of rates of general corrosion and maximum pitting penetration on concrete embedded steel reinforcement", *Cem. Concr. Res.*, **25**(2), 257-264. https://doi.org/10.1016/0008-8846(95)00006-2.

Hosseini, S.A., Shabakhty, N. and Mahini, S.S. (2015), "Correlation between chloride-induced corrosion initiation and time to cover cracking in RC Structures", *Struct. Eng. Mech.*, **56**(2), 257-273. http://dx.doi.org/10.12989/sem.2015.56.2.257.

Jamali, A., Angst, U., Adey, B. and Elsener, B. (2013), "Modeling of corrosion-induced concrete cover cracking: A critical analysis", *Construct. Build. Mater.*, **42**, 225-237. https://doi.org/10.1016/j.conbuildmat.2013.01.019.

Kent, D.C. and Park, R. (1971), "Flexural members with confined concrete", *J. Struct. Division Proc. American Soc. Civil Eng.*, **97**(ST7), 1969-199.

Khan, I., François, R. and Castel, A. (2014), "Prediction of reinforcement corrosion using corrosion induced cracks width in corroded reinforced concrete beams", *Cem. Concr. Res.*, **56**, 84-96. https://doi.org/10.1016/j.cemconres.2013.11.006.

Lee, H.S., Noguchi, T. and Tomosawa, F. (2002), "Evaluation of the bond properties between concrete and reinforcement as a function of the degree of reinforcement corrosion", *Cem. Concr. Res.*, **32**(8), 1313-1318. https://doi.org/10.1016/S0008-8846(02)00783-4.

Liu, Y. and Weyers, R.E. (1998), "Modeling the time-to-corrosion cracking in chloride contaminated reinforced concrete

structures", *ACI Mater. J.*, **95**(6), 675-681.
Malerba, P. G., Sgambi, L., Ielmini, D. and Gotti, G. (2017), "Influence of corrosive phenomena on bearing capacity of RC and PC beams", *Adv. Concrete Construct.*, **5**(2), 117-143. https://doi.org/10.12989/acc.2017.5.2.117.
Malumbela, G., Alexander, M. and Moyo, P. (2010), "Interaction between corrosion crack width and steel loss in RC beams corroded under load", *Cement Concrete Res.*, **40**(9), 1419-1428. https://doi.org/10.1016/j.cemconres.2010.03.010.
Mori, Y. and Ellingwood, B.R. (1993), "Reliability-based service-life assessment of aging concrete structures", *J. Struct. Eng.,* **119**(5), 1600-1621. https://doi.org/10.1061/(ASCE)0733-9445(1993)119:5(1600).
Rodriguez, J., Ortega, L., Casal, J. and Diez, J. (1996), "Corrosion of reinforcement and service life of concrete structures", *Durability Build. Mater. Components*, **1**(1), 117-126.
Stanish, K., Hooton, R.D. and Pantazopoulou, S.J. (1999), "Corrosion effects on bond strength in reinforced concrete", *ACI Struct. J.*, **96**(6), 915-921.
Vidal, T., Castel, A. and François, R. (2004), "Analyzing crack width to predict corrosion in reinforced concrete", *Cem. Concr. Res.*, **34**(1), 165-174. https://doi.org/10.1016/S0008-8846(03)00246-1.
Vidal, T., Castel, A. and Francois, R. (2007), "Corrosion process and structural performance of a 17 years old reinforced concrete beam stored in chloride environment", *Cem. Concr. Res.*, **37**(11), 1551-1561. https://doi.org/10.1016/j.cemconres.2007.08.004.
Vu, K.A.T, Stewart, M.G. and Mullard, J.A. (2005), "Corrosion-induced cracking: experimental data and predictive models", *ACI Struct. J.*, **102**(5), 719-726.
Vu, K.A.T., Mullard, J.A. and Stewart, M.G. (2000), "Structural reliability of concrete bridges including improved chloride-induced corrosion models", *Struct. Safety*, **22**(4), 313-333. https://doi.org/10.1016/S0167-4730(00)00018-7.
Yalsyn, H. and Ergun, M. (1996), "The prediction of corrosion rates of reinforcing steels in concrete", *Cement Concrete Res.*, **26**(10), 1593-1599. https://doi.org/10.1016/0008-8846(96)00139-1.
Zhang, R., Castel, A. and François, R. (2010), "Concrete cover cracking with reinforcement corrosion of RC beam during chloride-induced corrosion process", *Cem. Concr. Res.*, **40**, 415-425. https://doi.org/10.1016/j.cemconres.2009.09.026.
Zhou, H., Liang, X., Wang, Z., Zhang, X. and Xing, F. (2017), "Bond deterioration of corroded steel in two different concrete mixes", *Struct. Eng. Mech.,* **63**(6), 725-734. https://doi.org/10.12989/sem.2017.63.6.725.

CC